THE JOURNAL OF BIOLOGICAL CHEMISTRY
Vol. 277, No. 21, Issue of May 24, pp. 19095–19105, 2002

Printed in U.S.A.

Codon-Anticodon Interaction at the P Site Is a Prerequisite for tRNA Interaction with the Small Ribosomal Subunit*

Received for publication, September 14, 2001, and in revised form, February 25, 2002
Published, JBC Papers in Press, February 26, 2002, DOI 10.1074/jbc.M108902200

Markus A. Schäfer‡, A. Özlem Tastan‡, Sebastian Patzke, Gregor Blaha, Christian M. T. Spahn§, Daniel N. Wilson¶, and Knud H. Nierhaus‖

From the Max-Planck-Institut für Molekulare Genetik, AG Ribosomen, Ihnestrasse 73, D-14195 Berlin, Germany

The arrival of high resolution crystal structures for the ribosomal subunits opens a new phase of molecular analysis and asks for corresponding analyses of ribosomal function. Here we apply the phosphorothioate technique to dissect tRNA interactions with the ribosome. We demonstrate that a tRNA bound to the P site of *non-programmed* 70 S ribosomes contacts predominantly the 50 S, as opposed to the 30 S subunit, indicating that codon-anticodon interaction at the P site is a prerequisite for 30 S binding. Protection patterns of tRNAs bound to isolated subunits and *programmed* 70 S ribosomes were compared. The results suggest the presence of a movable domain in the large ribosomal subunit that carries tRNA and reveal that only ~15% of a tRNA, namely residues 30 ± 1 to 43 ± 1, contact the 30 S subunit of programmed 70 S ribosomes, whereas the remaining 85% make contact with the 50 S subunit. Identical protection patterns of two distinct elongator tRNAs at the P site were identified as tRNA species-independent phosphate backbone contacts. The sites of protection correlate nicely with the predicted ribosomal-tRNA contacts deduced from a 5.5-Å crystal structure of a programmed 70 S ribosome, thus refining which ribosomal components are critical for tRNA fixation at the P site.

Crystal structures for both 30 S (1, 2) and 50 S ribosomal subunits (3, 4) have been presented at molecular resolution, which has enabled certain ligand interactions with these subunits to be identified. On the 30 S subunit, interactions with initiation factors, numerous antibiotics (5–7), and tRNAs (8) have been determined, the latter of which has led to a detailed understanding of the mechanism of ribosome decoding at the A site. In addition to antibiotics, a transition state analogue for peptide bond formation, the "Yarus inhibitor," has been soaked into crystals of the large ribosomal subunit (9), the results of which have evoked intense discussion regarding the mechanism of peptide bond formation.

The highest resolution structure for a complete 70 S ribosome is currently at 5.5 Å (10). At this resolution, molecular interactions with bound ligands cannot be directly visualized; instead, they are inferred by modeling based on the high resolution subunit structures. This has enabled the path of the mRNA through the ribosome, encompassing 31 nucleotides from positions −15 to +16, to be determined (11), where the first nucleotide of the P site codon is defined as position +1. Furthermore, the positions of A, P, and E site tRNAs were determined allowing contacts with the ribosomal components to be predicted (10), which were in good agreement with previous studies of tRNA-ribosome interactions.

The general positions of tRNAs at the A, P, and E sites are well known from cryo-electron microscopy studies of functionally competent complexes (12), but at 11.5-Å resolution relatively little information pertaining to specific tRNA-ribosome interactions is available. Numerous chemical probing and cross-linking studies have been employed to map the contact sites on the rRNA from ribosome-bound tRNA (or analogs thereof; Refs. 13–15), but there are few comprehensive studies examining the reverse situation, namely protection of bound tRNAs by ribosomal components. One such study analyzed the protection against hydroxyl radical probing conferred by a 30 S subunit to a P site-bound tRNA. In this study the 30 S subunit shielded positions 28–46 (33% of the 76 positions) of the P site-bound $tRNA^{Phe}$, but a number of additional protections outside this region were observed, thus limiting the precise definition of the contact border of a tRNA bound to the small subunit. Little information is available regarding the protection pattern on a tRNA afforded by the 50 S subunit.

Here we present the first comprehensive study examining the protection patterns on tRNAs afforded by the 70 S ribosome as well as by 30 S and 50 S subunits. We demonstrate that, in the absence of codon-anticodon interaction at the P site of 70 S ribosomes, tRNA contacts on the ribosome are almost exclusively on the 50 S subunit, *i.e.* codon-anticodon interaction at the P site is a prerequisite for tRNA contacts with the 30 S subunit. Contact with the 30 S constitutes only 15% of the tRNA molecule, namely from position 30 ± 1 to 43 ± 1, whereas the 50 S subunit presents the majority of contact sites making up the remaining 85%. Furthermore, identical protection patterns result for two distinct elongator tRNAs, confirming that interaction between the tRNA and ribosomal components occur exclusively through conserved regions. Our data nicely complement the crystal structure reinforcing and extending the predicted contacts between ribosomal components and ribosome-bound tRNA.

EXPERIMENTAL PROCEDURES

The sources of chemicals and plasmids were as described in Ref. 16. Isolation of ribosomes and ribosomal subunits followed (17).

Preparation of mRNAs—The MF-mRNA[1] containing unique codons, one for Met and one for Phe, were obtained by *in vitro* T7-dependent

* This work was supported in part by Grant Ni 176/9-2 from the Deutsche Forschungsgemeinschaft (to K. H. N.). The costs of publication of this article were defrayed in part by the payment of page charges. This article must therefore be hereby marked "*advertisement*" in accordance with 18 U.S.C. Section 1734 solely to indicate this fact.

‡ Both authors contributed equally to this work.
§ Current address: Howard Hughes Medical Inst., Wadsworth Center, State University of New York, Albany, NY 12201-0509.

¶ Supported by the Alexander von Humboldt Foundation.

‖ To whom correspondence should be addressed. Tel.: 49-30-8413-1700; Fax: 49-30-8413-1594; E-mail: nierhaus@molgen.mpg.de.

[1] The abbreviation used is: MF-mRNA, mRNA containing a codon for Met (M) and Phe (F).

TABLE I
Interference experiments with tRNA^{Phe} bound to ribosomal subunits or 70 S ribosomes in the presence of poly(U)

The experimental strategy (see text) ensures that a band is missing or weakened on the sequencing gel when a thioate at a distinct position prevented binding of tRNA. In this case, the ratio (intensity of a band in the bound state/intensity of the corresponding band in solution) is smaller than 1. Bold numbers, ratios ≤ 0.55; underlined numbers, ratios from 0.56 to 0.75; the standard deviation was below 10%. ND, not determined.

	70 S	50 S	30 S
1G	ND	ND	ND
2C	ND	ND	ND
3C	ND	ND	ND
4C	ND	ND	ND
5G	1.37	0.90	1.10
6G	1.01	1.05	1.14
7A	0.65	0.83	1.02
8U	0.96	0.98	0.81
9A	**0.55**	0.64	1.02
10G	1.01	1.01	1.15
11C	0.85	0.90	0.99
12U	1.10	1.00	0.95
13C	0.84	0.94	0.88
14A	0.92	1.11	1.20
15G	0.83	0.85	1.09
16U	1.00	0.98	0.93
17C	1.01	1.02	0.90
18G	1.10	0.81	1.16
19G	0.88	0.81	1.04
20U	1.64	1.15	0.90
21A	0.65	0.69	1.32
22G	0.90	0.84	1.28
23A	0.88	0.93	0.97
24G	1.19	0.99	1.15
25C	0.85	0.96	0.81
26A	0.98	1.19	1.12
27G	0.96	1.02	1.30
28G	1.04	1.03	1.30
29G	1.05	1.03	1.18
30G	1.01	0.96	1.03
31A	1.01	1.09	1.14
32U	0.88	0.88	1.18
33U	0.75	1.19	**0.55**
34G	0.81	1.05	1.12
35A	**0.42**	1.06	0.68
36A	**0.51**	0.97	0.61
37A	0.62	0.90	0.70
38A	0.75	0.98	0.79
39U	1.02	1.06	1.08
40–43C	0.89	0.99	0.93
44G	0.75	0.90	1.30
45U	0.85	0.96	1.02
46G	0.69	0.72	0.97
47U	0.85	0.96	1.02
48C	0.87	0.72	0.99
49C	0.80	0.74	0.93
50U	0.88	0.83	1.16
51U	0.96	1.03	1.16
52G	0.95	1.03	1.16
53G	0.95	1.03	1.16
54U	0.93	0.82	1.05
55U	1.14	1.14	1.25
56C	0.90	1.02	1.05
57G	1.33	0.88	1.32
58A	1.01	0.83	1.11
59U	0.86	1.01	1.16
60U	0.86	1.01	1.16
61–62C	0.89	0.85	0.96
63G	0.95	1.00	1.15
64A	0.86	0.81	1.09
65G	0.95	1.00	1.15
66U	0.71	0.89	0.96
67C	ND	ND	ND
68C	ND	ND	ND
69G	ND	ND	ND
70G	ND	ND	ND
71G	ND	ND	ND
72C	ND	ND	ND
73A	ND	ND	ND
74C	ND	ND	ND
75C	ND	ND	ND
76A	ND	ND	ND

run-off transcription. The oligonucleotide 5′-GGGAAAAGAAAA-GAAAAGAAA**AUGUUC**AAAAGAAAAGAAAAGAAAU-3′, which does not possess any predictable secondary structure, was inserted in a ptz43 plasmid directly behind a class III T7 promoter. Transcription of *Ssp*I linearized plasmid DNA was done according to the standard conditions for *in vitro* transcription assay (16), with an exception that the final concentration of UTP was reduced by one tenth (to 0.375 mM) to prevent secondary product formation. Purification was performed by loading the transcription mix on 8% polyacrylamide gel (acrylamide/bisacrylamide: 19/1). After electrophoresis the band corresponding to the full-length mRNA was cut out and phenol-extracted (5 ml of phenol and 5 ml of extraction buffer containing 10 mM Tris-HCl, pH 7.8, 100 mM NaCl, 1% SDS, 1 mM dithioerythritol). RNA was recovered from the aqueous phase by EtOH precipitation.

Poly(U) from Roche Molecular Biochemicals is not of uniform length. Fractionation of poly(U) (100 mg, 2462 A_{260}, in 3 ml of double-distilled H_2O) by gel filtration on Sephacryl S-400 HR (column: 65 cm length, 3 cm diameter; buffer: 300 mM sodium acetate with pH 5.5 at 4 °C, 2% MeOH) was performed, and the smallest fraction (50 ± 25 bases) was used in the experiments testing the tRNA conformations on the ribosome under various buffer conditions.

Preparation of Thioated tRNAs—The thioated and non-thioated tRNA^{Phe} and tRNA^{Met} were obtained by *in vitro* T7-dependent run-off transcription from suitable plasmids (for tRNA^{Phe}, pSTtPhe, and for tRNA^{Met}, pSTMetM; both plasmids are derivatives of pSP65) after linearizing them with *Bst*NI or *Ssp*I, respectively (16). Purification of the transcripts was achieved by using the Qiagen RNA/DNA Midi kit.

Complex Formation—The binding of transcribed deacyl-tRNAs to the ribosomal P site and to the ribosomal subunits was performed under either polyamine (20 mM Hepes/KOH, pH 7.8 (0 °C), 6 mM $MgCl_2$, 150 mM NH_4Cl, 2 mM spermidine, 0.05 mM spermine, and 4 mM 2-mercaptoethanol) or conventional buffer conditions (20 mM Hepes/KOH, pH 7.8 (0 °C), 10/20 mM $MgCl_2$, 100 mM NH_4Cl). Complex formation for the subunit experiments was achieved during an incubation of 50 pmol of tRNA^{Phe} together with 50 μg of poly(U) mRNA and 60 pmol of ribosomes or ribosomal subunits for 10 min at 37 °C. 70 S complexes with or without mRNA were established essentially under the same conditions with tRNA^{Phe} or tRNA$_m^{Met}$ ± the respective mRNA, *i.e.* 50 μg of poly(U) (tRNA^{Phe}) or 360 pmol of MF-mRNA (tRNA$_m^{Met}$). Binding of tRNAs to 70 S ribosomes or to either subunit was performed with less than 1 tRNA/ribosome to ensure site specificity; the binding values were 0.3 ± 0.1 tRNA bound/ribosome or 30 S subunit (input of tRNA:(70 S or subunit) = 0.8:1). As previously described the 50 S binding values were significantly lower (18) and amounted to 0.12 ± 0.02 (note that a possible 30 S contamination of the 50 S preparation was below 1% and thus could be responsible for maximally 0.003 of the bound tRNA per 50 S subunit). For interference experiments the complexes were isolated, and the tRNA extracted and subjected to an iodine treatment. Those bands that are reduced in their intensities as compared with the corresponding bands of a tRNA in solution indicated an interference of tRNA binding via thioation of the corresponding phosphate. For accessibility (protection) experiments, the complexes were treated with iodine before the tRNA and/or tRNA fragments were isolated and subjected to sequencing analysis.

Iodine Cleavage Experiments—The procedure was as described in Ref. 19. Non-phosphorothioated transcribed tRNA was used as control and was not cleaved by iodine.

Quantitative Analysis—13% denaturing polyacrylamide sequencing gels (acrylamide/bisacrylamide: 19/1, 7 M urea; 10,000–30,000 dpm/lane) were exposed for 12 h-16 h on a PhosphorImager™ (Molecular Dynamics) prior to classical autoradiography on x-ray films. Evaluation of the scanned gel was performed with the package program Image-

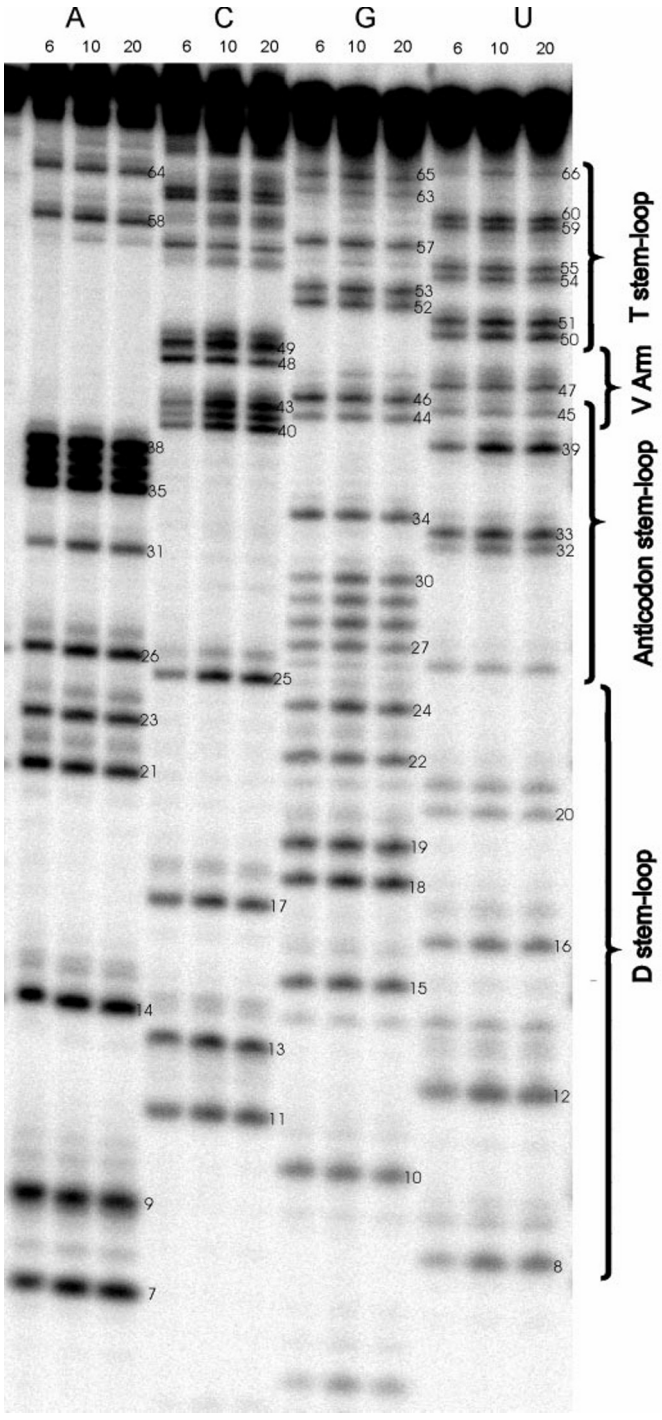

FIG. 1. **Sequencing gel of protection experiments with thioated tRNA^{Phe}.** tRNA^{Phe} was either in a buffer containing 6 mM Mg^{2+} and polyamines or a conventional buffers with 10 and 20 mM Mg^{2+} without polyamines (*lanes* marked with *6*, *10*, and *20*, respectively). The *numbers* next to the *bands* indicate the nucleotide positions, structural elements of the tRNA are indicated on the right-hand side.

Quant™ version 3.3 (Molecular Dynamics).

The experiments were repeated up to four times, and the data were normalized as follows. Assuming that the results of two experiments performed under identical conditions are considered, the first normalization concerned variation in loading between respective thio-A-lanes (input normalization). Here the total counts of the two lanes were normalized, and the intensity of each band was multiplied by the normalization factor. Input normalization was performed for both complex and solution cleavage experiments individually. The second normalization is between the two sets of data (bound tRNA *versus* tRNA in solution) and essentially followed an identical procedure, where the protection value regarding the amount of $tRNA_{bound}/tRNA_{solution}$ for a distinct band was calculated using the normalized intensities of corresponding bands derived from a tRNA in a complex and a tRNA in solution, respectively.

RESULTS

Interference of tRNA Ribosome Binding Ability because of Site-specific Thioation—In the following sets of experiments, we apply a phosphorothioate technique to define the environment of a P site-bound tRNA on the ribosome. The phosphorothioate technique (16, 20) requires the replacement of a nonbridging oxygen atom of a phosphate group with a sulfur atom in the tRNA backbone. The importance of the method relies on the fact that the small and relatively inert iodine molecule (I_2) triggers cleavage of the sugar-phosphate backbone with an efficiency of ~5% at the thioated site, and that this cleavage can be prevented by tight contacts, *e.g.* with the ribosomal matrix. If the thioated tRNA is 5′-labeled with ^{32}P, the "accessibility" or "protection" pattern can be assessed for most of the phosphate positions of a tRNA on a sequencing gel (footprinting experiment).

Usually replacement of the oxygen atom with a sulfur atom does not affect the functional spectrum of a molecule. Thioated tRNA transcripts have been shown to be active in aminoacylation, ternary complex formation, and poly(Phe) synthesis (16). However, at certain positions such a replacement can interfere with the binding of a tRNA to a ribosomal site, *e.g.* by changing the tRNA structure or by removing an oxygen atom of the phosphate group that was involved in the coordination of a Mg^{2+}. This in itself can provide interesting insights into the functional importance of the certain phosphate groups. Furthermore, it is essential to determine these positions before undertaking further analyses.

Interference by thioation of tRNA binding was determined as described under "Experimental Procedures." Put simply, tRNAs that exhibit interference, *i.e.* have a reduced ribosome binding ability because of thioation at distinct sites, can be identified by iodination *after* extraction of the tRNAs from the ribosome complexes. Bands corresponding to interference sites will be weaker than the corresponding bands of a control tRNA solution pattern.

In Table I the interference values for positions 5–66 of tRNA^{Phe} have been compiled. An interference value of 1.0 correlates with no interference, whereas a value of 0 would correlate with total interference. Interference values are divided into weak (underlined values between 0.56 and 0.75) and strong (bold values ≤ 0.55). On the 70 S ribosome, weak interference was found at the phosphate positions A7, A21, U33, A37, A38, G44, G46, and U66, but still allowed assessment of the protection pattern. In contrast, strong interference was observed at the positions A9, A35, and A36, preventing any protection analysis at these positions. The tRNA interference patterns obtained using ribosomal subunits were qualitatively very similar to those observed with the 70 S at each respective position. Exceptions were at positions A7, G44, and U66, where modification interfered with tRNA binding to 70 S ribosomes, but not to 50 S subunits. Schnitzer and von Ahsen (21) identified phosphate positions 33, 35, and 36, which, when thioated, prevented tRNA binding to the 30 S subunit. We have identified the same positions for 30 S subunit interference and, in addition, position 37.

The Protection Pattern of a tRNA Bound to the P Site of a 70 S Ribosome Is Not Significantly Affected by Changes in Buffer Composition—tRNA locations on the ribosome are highly sensitive to buffer conditions. This has been illustrated by cryo-electron microscopy, where P site-bound deacylated tRNA under both polyamine and conventional buffers was examined

TABLE II
Accessibility pattern of thioated tRNA^{Phe} under various buffer conditions

A6, accessibility under polyamine conditions (6 mM Mg^{2+}); A10 and A20, accessibility under conventional buffer conditions without polyamines at 10 and 20 mM Mg^{2+}, respectively; bold numbers, the intensity ratio of the corresponding bands is below 0.49 (*e.g.* A7, 0.43 for A6/A10 means that the accessibility of phosphate at position A7 is protected more under polyamine buffer conditions than under conventional buffer conditions); italicized numbers, the ratio is between 0.5 and 0.79; underlined numbers, the ratio is above 1.15; ratios between 0.8 and 1.14 are not considered to differ significantly. The numbers are averages of up to four experiments, the standard deviation was below 10%. ND, not determined.

	A6/A10	A6/A20	A10/A20
1G	ND	ND	ND
2C	ND	ND	ND
3C	ND	ND	ND
4C	ND	ND	ND
5G	ND	ND	ND
6G	ND	ND	ND
7A	**0.43**	**0.39**	0.90
8U	**0.31**	**0.34**	1.10
9A	*0.76*	*0.75*	0.98
10G	*0.70*	0.82	1.17
11C	**0.44**	0.63	1.45
12U	**0.41**	**0.37**	0.92
13C	**0.45**	*0.54*	1.22
14A	*0.54*	*0.54*	1.00
15G	*0.61*	*0.72*	1.17
16U	**0.38**	**0.36**	0.94
17C	*0.58*	*0.63*	1.09
18G	*0.63*	*0.70*	1.12
19G	*0.65*	*0.75*	1.14
20U	*0.61*	*0.57*	0.94
21A	0.87	0.91	1.04
22G	*0.64*	*0.72*	1.13
23A	*0.63*	*0.57*	0.91
24G	**0.36**	**0.49**	1.35
25C	**0.29**	**0.35**	1.22
26A	**0.46**	**0.43**	0.94
27G	*0.55*	*0.67*	1.23
28G	**0.36**	**0.42**	1.16
29G	**0.33**	**0.35**	1.06
30G	**0.27**	**0.27**	1.02
31A	**0.31**	**0.34**	1.08
32U	**0.34**	**0.39**	1.14
33U	**0.45**	*0.50*	1.12
34G	*0.70*	0.94	1.34
35A	*0.72*	0.82	1.14
36A	0.85	0.85	1.00
37A	*0.76*	*0.79*	1.03
38A	*0.67*	*0.68*	1.02
39U	**0.29**	**0.31**	1.05
40C	**0.46**	*0.59*	1.27
41C	**0.38**	*0.55*	1.43
42–43C	**0.39**	*0.57*	1.49
44G	*0.78*	0.92	1.18
45U	1.07	0.96	0.90
46G	1.01	1.18	1.17
47U	0.88	0.80	0.90
48C	1.16	1.28	1.10
49C	*0.70*	0.91	1.30
50U	**0.47**	**0.45**	0.96
51U	*0.51*	*0.51*	1.00
52G	*0.77*	1.13	1.47
53G	*0.60*	*0.78*	1.30
54U	*0.63*	*0.71*	1.13
55U	0.85	0.84	0.99
56C	1.12	1.31	1.17
57G	*0.51*	*0.67*	1.31
58A	*0.64*	*0.66*	1.04
59U	*0.58*	*0.56*	0.96
60U	*0.60*	*0.60*	1.02
61C	1.04	1.13	1.09
62C	0.88	0.95	1.09
63G	*0.61*	*0.69*	1.13
64A	*0.77*	*0.71*	0.93
65G	**0.46**	*0.58*	1.25
66U	**0.45**	**0.48**	1.06
67C	ND	ND	ND
68C	ND	ND	ND
69G	ND	ND	ND
70G	ND	ND	ND
71G	ND	ND	ND
72C	ND	ND	ND
73A	ND	ND	ND
74C	ND	ND	ND
75C	ND	ND	ND
76A	ND	ND	ND

(22). In the polyamine buffer the tRNA was mainly present in the canonical P site, whereas in the conventional buffer the deacylated tRNA was exclusively found in the hybrid site P/E of programmed ribosomes (22). Based on this observation, we were interested to test whether there is a significant difference in the protection patterns of a deacylated tRNA, free in solution and bound to the ribosomal P site (P_i state, i for initiation-like, *i.e.* free A and E sites), under polyamine or conventional buffer conditions.

Fig. 1 shows a representative footprinting gel for a deacylated tRNA^{Phe} in solution under different buffer conditions. We have chosen a polyamine system that allows, at Mg^{2+} concentrations below 10 mM, quantitative occupation of the tRNA binding sites and protein synthesis with a performance similar to *in vivo* perfection (for discussion, see Ref. 23). In contrast, conventional buffer systems do not allow quantitative occupation of the ribosomal tRNA binding sites at Mg^{2+} concentrations below 10 mM (24). Furthermore, because Mg^{2+} concentrations above 20 mM do not support protein synthesis, we chose to compare conventional buffers containing Mg^{2+} concentrations at these boundaries, namely 10 and 20 mM.

Little discernable difference was observed between the protection patterns under conventional buffer conditions at 10 or 20 mM Mg^{2+} (*lanes 10* and *20* according to 10 and 20 mM Mg^{2+}, respectively), whereas the intensities at a number of positions generated under polyamine-buffer (*lanes 6*) differ from the corresponding ones at conventional conditions. For example, bases C40–C43 are weaker than the corresponding bands in the 10 and 20 mM Mg^{2+} lanes. Quantitative analyses of four such experiments were averaged, and the results are presented in Table II. Generally, phosphates located in the tRNA loops were equally accessible to iodine-induced cleavage under all buffer conditions tested, *e.g.* bases of the anticodon loop G34–A38 and those of the D loop A14–A21, whereas phosphates located in many helical regions were less accessible under polyamine conditions, *e.g.* phosphates of the anticodon stem G28–A31 and U39–C43. The accessibility of a few bases was magnesium concentration-dependent, *e.g.* C49 and G53 were more accessible under conditions of 10 mM Mg^{2+} than 20 mM.

A pattern specifically resulting from protections by the ribosome matrix was assessed by normalization against the "background" protection that results in the absence of ribosome, *i.e.* in the corresponding buffer solution only. Thus, the difference pattern generated represents specifically the protections of a tRNA by the ribosome. Surprisingly, the difference patterns were remarkably similar to one another regardless of the buffer condition used. The difference patterns showed strong global protection of the bound tRNA similar to previous observations

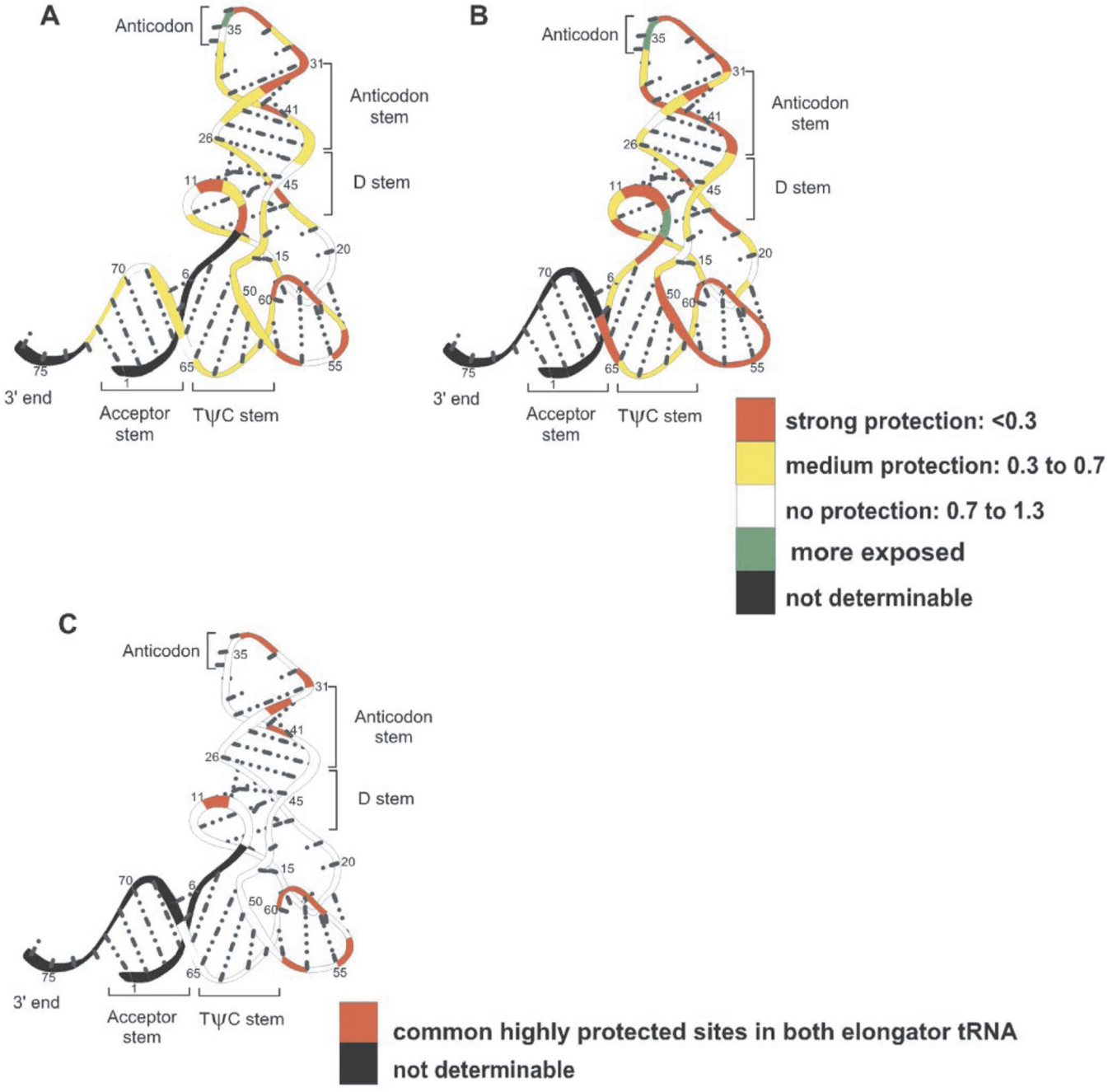

FIG. 2. **Comparison of accessibility patterns of** $tRNA_m^{Met}$ **(*A*) and** $tRNA^{Phe}$ **(*B*) at the P site of 70 S ribosomes programmed with MF-mRNA and poly(U), respectively.** These experiments were performed in polyamine buffer. *C*, strongly protected phosphates in both $tRNA^{Phe}$ and $tRNA_m^{Met}$ (*red*).

(Ref. 16; see also Fig. 2*B*). However, there were a few exceptions; A31, C49, C61, and C62 showed less protection under conventional buffer conditions than polyamine, and one strand of the anticodon stem, U39–G46, was less protected, specifically, under 20 mM Mg^{2+} buffer conditions.

Similar Protection Patterns Are Derived Using Distinct tRNA Species—To test whether the protection pattern at the P site with deacylated $tRNA^{Phe}$ is specific for $tRNA^{Phe}$ species or whether it is representative for all tRNA species, the protection experiments for a completely distinct elongator tRNA were performed. The tRNA chosen was elongator $tRNA_m^{Met}$, as it differs in sequence from $tRNA^{Phe}$ at 28 of 76 comparable positions (37%).

Experiments were performed with $tRNA_m^{Met}$ as described for $tRNA^{Phe}$, the results of which were converted into a color code as shown in Fig. 2 (*A* and *B*) ($tRNA_m^{Met}$ and $tRNA^{Phe}$, respectively), where varying degrees of protection are represented by different colors. The protection pattern of $tRNA_m^{Met}$ is in general agreement with that of $tRNA^{Phe}$, although it displays overall weaker protection. The extra arm and the D loop are only weakly protected, or not at all. In both tRNAs, parts of the TΨC and D-stem and the anticodon loops are strongly protected. Although the regions with strong protection comprise both paired and unpaired bases, they are predominantly found within exposed regions of the tertiary structure of the tRNA (Fig. 2*C*). The accessibility at position 66 discriminates both tRNA species; this position exhibits strong protections in 70 S ribosomes (and 50 S subunits, data not shown) with $tRNA^{Phe}$,

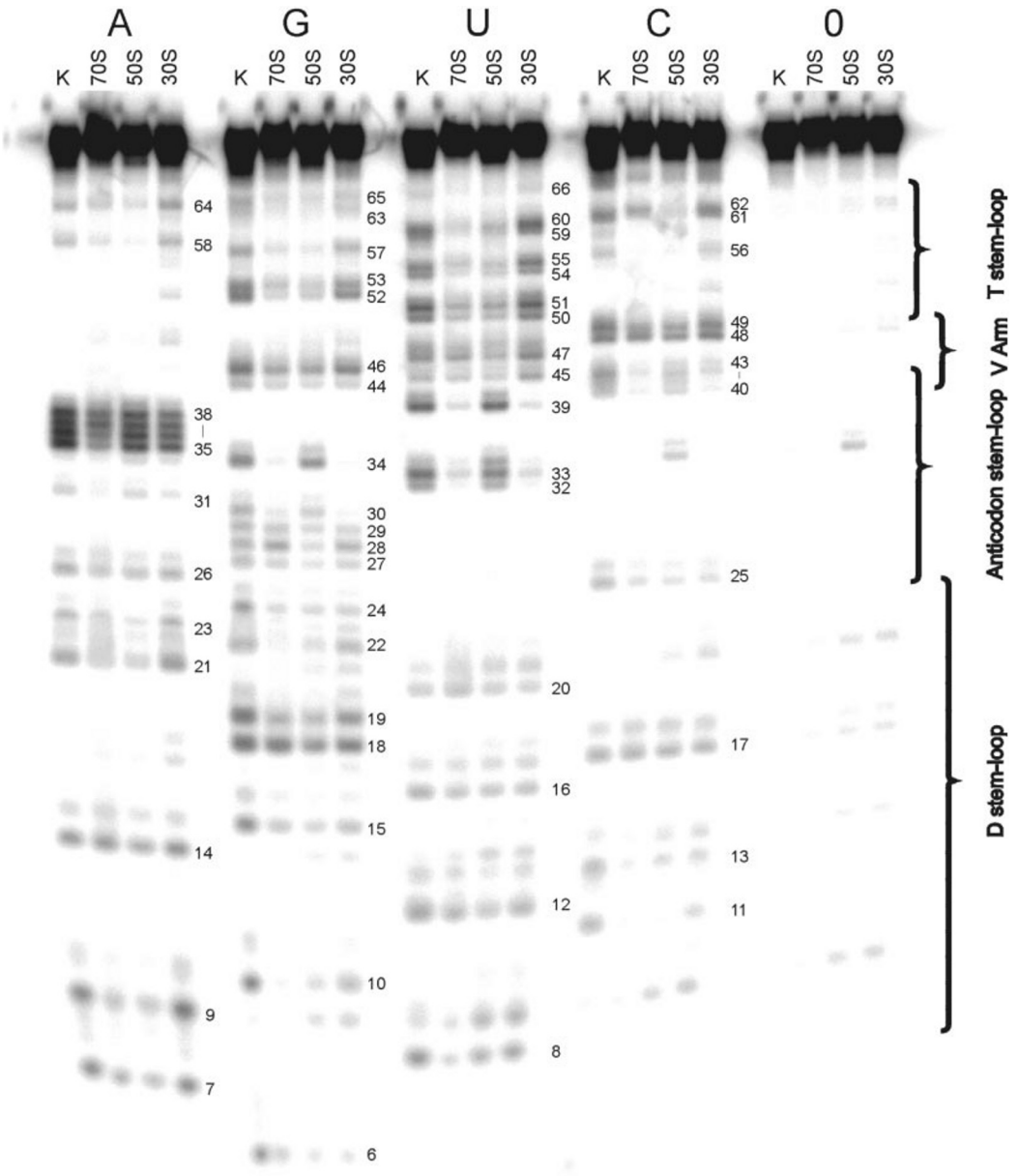

FIG. 3. **Sequencing gel of a protection experiment with thioated tRNA^{Phe} bound to programmed 70 S ribosomes or 30 or 50 S subunits.** A weakened intensity of a band in comparison to the respective control reflects a protection by the ribosomal complex. *K*, cleavage pattern of tRNAs in solution. The *numbers* indicate the nucleotide positions; on the *right side* structural elements of the tRNA are indicated.

but is very accessible with tRNA$_m^{Met}$ (Fig. 2, compare *A* and *B*).

30 and 50 S Subunit tRNA Protections Are Additive and Equate with the Protection Pattern Afforded by the P Site of Complete 70 S Ribosomes—In an attempt to define the 70 S protection pattern in terms of the component subunit boundaries, thioated tRNA^{Phe} was bound to 30 and 50 S subunits and the respective protection patterns generated were compared with that for the complete 70 S (a representative gel is shown in Fig. 3). Multiple gels were scanned and normalized, and the protection pattern of tRNA^{Phe} bound to programmed 30 S and to 50 S subunits was compared with that seen at the P site of programmed 70 S ribosomes in Fig. 4, *A* and *B*, respectively. Strikingly, the results show that the region 30 ± 1 to 43 ± 1 is protected in 30 S subunits and 70 S ribosomes in an almost identical fashion, whereas the regions outside this sequence are clearly less protected in the 30 S subunits. A complementary picture is found when the 50 S protection pattern in the 50 S subunit is compared with the 70 S ribosome, *i.e.* no correspondence of protections between sequences 29 and 43, and instead good agreement outside of this region.

Addition of mRNA Results in Additional Protection of the Anticodon Stem-loop of a P Site-bound tRNA—The protection pattern of tRNA^{Phe} was determined in the presence and absence of mRNA. The results are presented graphically, where the *x* axis represents the positions of the phosphate residues of tRNA^{Phe} (theoretically 1–76), and the *y* axis the relative accessibility for each position (Fig. 5, *A* and *B*). Upon addition of mRNA, there is a conspicuous change in protection extending between positions 29 and 39. This region of protection corresponds with the anticodon stem-loop and three additional bases of the 3′-strand of the anticodon stem. Positions prior to 28 and those subsequent to position 40 exhibit protection patterns that remain unaltered in the presence or absence of poly(U). Exceptions include bases A26, C48, and C61/62 (the latter could not be separated in the sequencing gel). Our results are in good agreement with similar experiments performed with tRNA$_m^{Met}$ in the presence and absence of the heteropolymeric MF-mRNA, an mRNA containing a unique AUG codon (25). Furthermore,

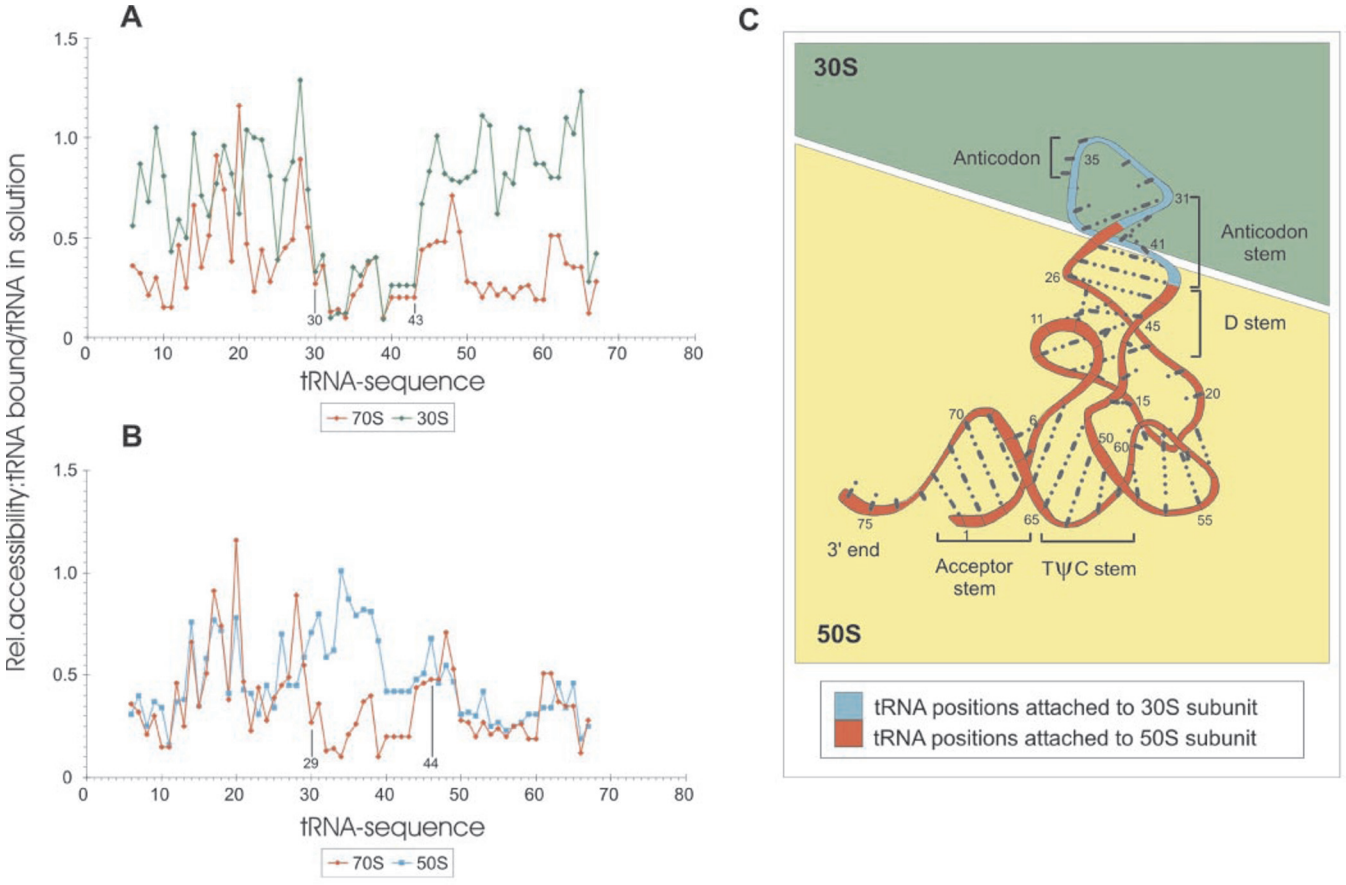

FIG. 4. **Protection graphs of tRNA^{Phe} bound to programmed 70 S ribosomes and 30 and 50 S subunits (the corresponding sequencing gel is seen in Fig. 3).** *A*, comparison of the protection pattern with 30 S subunits (*green*) and that with 70 S ribosomes (*red*). *B*, comparison of the protection pattern with 50 S subunits (*blue*) and that with 70 S ribosomes (*red*). *C*, the regions of a deacylated tRNA at the P site of 70 S ribosomes being in contact with the small (*blue*) or large ribosomal subunit (*red*). Note that the terms "protection" and "accessibility" describe the same phenomenon, except in a reciprocal fashion, *i.e.* a high accessibility of a phosphate residue correlates with low protection and *vice versa*.

protection of tRNA^{Phe} was assessed in the presence of the non-cognate poly(A) mRNA, which exhibited a pattern identical to that obtained in the absence of mRNA (data not shown), thus reflecting the specificity of the system.

DISCUSSION

Polyamines Contribute to the Stability of the tRNA Tertiary Structure—We demonstrate via iodine cleavage of phosphorothioated tRNAs that, in solution, tRNAs adopt different conformations under polyamine and conventional buffer conditions. Under conventional buffer conditions a Mg^{2+} shift from 10 to 20 mM had no significant influence on tRNA conformation. In contrast to conventional buffers, strong protection using polyamine buffer was seen, for example, at the phosphate groups of the anticodon stem (24–26 and 39–43) and around phosphate 10 (residues 7, 8, and 11–13; see Table II). This suggests that, despite the low Mg^{2+} concentration, the tRNA tertiary structure in the polyamine buffer is more compact and stable than in the conventional buffer system with 10–20 mM Mg^{2+}. This is surprising, as the general wisdom is that RNA structure becomes more stable at higher Mg^{2+} concentrations. This indicates that polyamines not only compensate for the lower magnesium, but also rather induce a more compact structure, a feature that might be related to the near *in vivo* performance of protein synthesis under polyamine conditions, in contrast with the conventional buffer systems (for review, see Ref. 23).

Interestingly, the regions of increased protection in polyamine buffer locate in the vicinity of two polyamine binding sites. In a crystal structure of yeast tRNA^{Phe}, besides four distinct Mg^{2+} ions, two spermine molecules are found. The first is located in the major groove at one end of the anticodon stem (phosphates 25, 26, and 41–43), and the second is near the variable loop and curls around phosphate 10 in a region where the polynucleotide chain takes a sharp turn (26). Because the differences in protection between the polyamine system and the conventional systems accumulate at the polyamine binding sites, we conclude that many of these additional protection sites can be attributed to the bound polyamines, thus underlining not only the impact of polyamines on RNA stabilization, but also the sensitivity of the phosphorothioate technique.

Refining the Ribosomal Components Responsible for Fixation of a tRNA at the P Site—The reduction in the accessibility of the phosphate groups of an AcPhe-tRNA located at the P site (16, 19) can be convincingly correlated with the points of contact between the ribosomal matrix and a P site fMet-tRNA as revealed by cryo-electron microscopy (27).

Here we analyze deacylated tRNA, and find that the protection patterns obtained with deacylated tRNAs bound to individual ribosomal subunits complement each other so as to equate with the pattern observed when a tRNA is bound to the P site of a 70 S ribosome. This observation allows a sharp delineation of the tRNA contact regions within the 70 S ribosome that are contributed by each of the component subunits. The small subunit contacts include the anticodon loop and the first two base pairs of the adjacent anticodon stem (positions 30 ± 1 to 43 ± 1), whereas the remaining 85% of the tRNA is

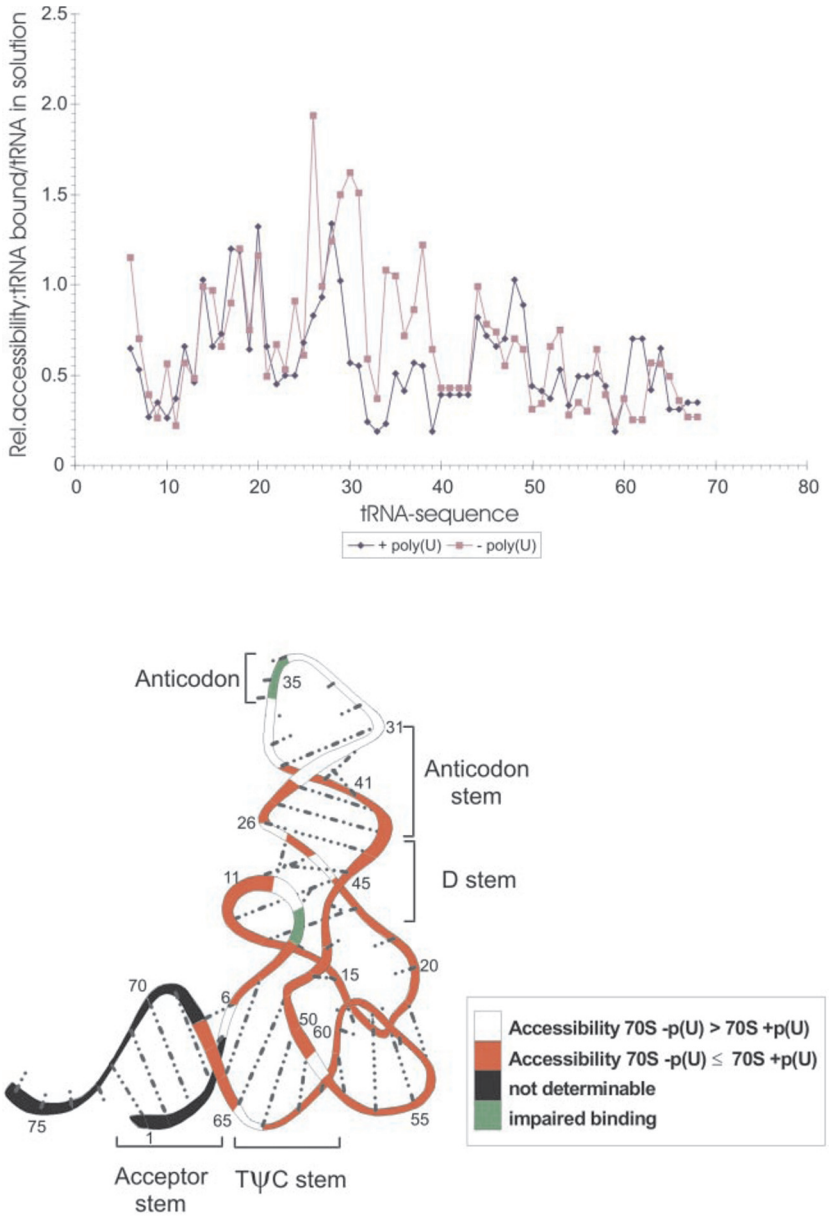

FIG. 5. **Influence of the mRNA on the binding pattern of tRNA^{Phe} at the P site of 70 S ribosomes.** *A*, "protection graph" showing the nucleotide positions of the tRNA^{Phe} on the *x* axis and the relative accessibility on the *y* axis. The pattern in the presence of poly(U) is shown in *blue* and that in the absence of mRNA in red. *B*, the data of *A* are projected onto the tertiary structure of tRNA^{Phe} using the following color code. *White*, the accessibility is reduced by at least 40% in the presence of mRNA; *red*, accessibility in the presence of poly(U) is greater than or equal to the accessibility in the absence of poly(U); *green*, thioation interferes with the binding of tRNA; *black*, not determinable.

in contact with the large subunit (Fig. 4*C*). The contribution of each subunit to the overall distribution of contacts made with the P site tRNA is in remarkable concordance with the 5.5-Å map of the tRNA·70 S complex (see Table III in Ref. 10) and also with the mimic of an anticodon-stem loop structure in the crystal of 30 S subunit (28). Fig. 6 illustrates the excellent agreement of our data with the 5.5-Å map of a 70 S complex; the 30 S protections of the anticodon stem-loop structure (positions 30 ± 1 to 41 ± 1 in *yellow*) are located exclusively in the neighborhood of 30 S components (*gold* and *red*) of the 70 S map, whereas the remaining portion of the tRNA (*dark blue*) lies within the domain of the 50 S subunits (*cyan* and *green*).

Furthermore, we have determined a number of strong protections that are common between two different species of elongator tRNA, namely tRNA^{Phe} and tRNA^{Met}. We believe that these phosphates may represent strategic fixation points on a deacylated tRNA at the P site. If this were so, then one could expect conservation of the tRNA bases adjacent to these phosphates and conservation of the neighboring ribosomal components. Indeed, this is the case. Eight of 10 strong protections are adjacent to conserved bases of the tRNA (Table III), and a detailed inspection of the 5.5-Å map of the 70 S complex revealed that the ribosomal components neighboring the 10 tRNA bases are remarkable conserved (Table IV). The rRNA bases are conserved in >95% bacteria and 80–100% across all three phylogenetic domains. Furthermore, we identify a number of conserved positions of ribosomal proteins that neighbor these phosphates, for example, position 120 (*E. coli* numbering)

TABLE III
Strongly protected bases in both tRNA^{Phe} and tRNA$_m^{Met}$

+, universally conserved base; R, purine; Y, pyrimidine (universally semiconserved).

Protected phosphate	Upstream nucleoside (toward 5′ end)	Downstream nucleoside (toward 3′ end)
11	G10	+ Y11
30	G29	G30
32	A31	+ Y32
34	+ U33	G34
41	C40	C41
54	+ G53	+ T54
56	+ Ψ55	+ C56
58	+ R57	+ A58
59	+ A58	U59
60	U59	+ Y60

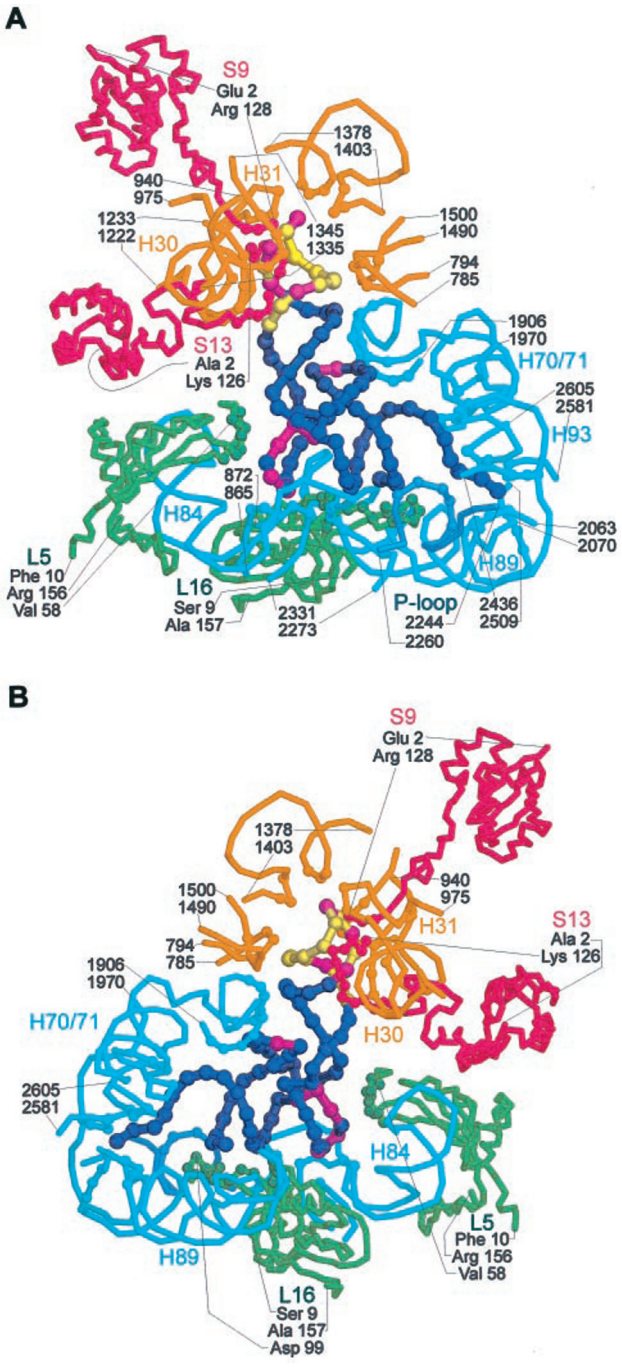

FIG. 6. **tRNA neighborhoods at the ribosomal P site of the 70 S ribosome according to Ref. 10 (see also Table IV).** *A*, view from the A site; *B*, view from the E site. tRNA: *yellow*, contacts with the small subunit; *blue*, contacts with the large subunit; *pink*, strongly protected sites in both $tRNA^{Phe}$ and $tRNA_m^{Met}$ at the P site (see Fig. 2*C*). Regions of the ribosomal components that are within a 10-Å radius of the P site tRNA are indicated with *spheres*. 30 S components: *gold*, 16 S rRNA; *red*, S-proteins. 50 S components: *cyan*, 23 S rRNA; *green*, L-proteins.

of S13 is always a Lys or an Arg residue and lies next to tRNA base G30, a highly conserved Arg-128 neighbors tRNA base Y32 and positions Arg/Lys-56 and Arg/Lys-64 of L5 are in close proximity to C56. This further corroborates the suggestion that the identified tRNA nucleotides are of strategic importance for tRNA fixation at the P site.

Identification of a Mobile Ribosomal Domain Associated with tRNA Transport—Although the protection experiments present a "static" picture of the ribosome, which is exemplified by the identification of fixation of the P site tRNA as described in the previous section, a comparison of protection patterns under different conditions and between different states enables an interpretation of two dynamic features of the ribosome.

First, the protection patterns afforded by isolated 30 S and the 50 S subunits could be combined to reconstruct the P site pattern of 70 S ribosomes. Isolated 30 S subunits have a single binding site, the prospective P site after association with the large subunit, as demonstrated with binding experiments (18) and via the toeprinting method (29). In contrast, isolated *E. coli* 50 S subunits bind exclusively deacylated tRNA to the E site and have no available P or A site (18, 30). The fact that the 50 S E site pattern is practically the same as the 50 S part of the 70 S P site pattern seems to be reminiscent of a P/E hybrid site of the hybrid site model for elongation, where the tRNAs are thought to creep through intermediary hybrid sites (A/P and P/E) before arriving, after translocation, at the classical P and E sites (Ref. 31; see also Ref. 32 for review). However, the similarity with a hybrid site does not hold here, because the 70 S P site pattern was obtained under polyamine-buffer conditions, where the tRNA is found in a canonical P site (22).

We note that a similar conservation in protection patterns was observed between pre- and post-translocation complexes (PRE and POST, respectively), with a deacylated tRNA at the P site in the PRE state and at the E site in the POST state. This led to the α-ϵ model for the ribosomal elongation cycle (reviewed in Ref. 23), which proposes the existence of a movable domain that binds and guides tRNAs during translocation. The movable domain contains two binding regions, α and ϵ, each of which bind a tRNA with a characteristic protection pattern. During translocation, the α-region carries a tRNA from the A to the P site and the ϵ-region a tRNA from the P to the E site.

Our finding that the protection pattern of a tRNA bound to isolated 50 S subunits (E site) is the same as that of the 50 S part of the 70 S P site can be interpreted in the frame of the α-ϵ model to suggest that the ϵ-part of the mobile tRNA carrier is at the E site in isolated 50 S subunits, but "swings" into the P site upon association with the 30 S subunit forming 70 S ribosomes.

Second, the accessibility pattern of a deacylated thioated tRNA in the P site of programmed ribosomes is almost identical under polyamine and conventional buffer conditions. However, it is known from cryo-electron microscopy that the locations of the tRNA are strikingly different, *i.e.* a deacylated tRNA is found at a classical P site under polyamine conditions and at a P/E hybrid site under conventional conditions (12). This suggests that the ribosomal components that hold the 50 S portion of the tRNA are located in a classical P site under polyamine conditions but slip into the E site position under conventional buffer conditions. The physiological relevance of the latter finding is immediately compromised by the buffer conditions themselves, *i.e.* their non-physiological nature (see Ref. 23 for discussion), but may nevertheless provide some insight into the mechanism of translocation.

In the frame of the α-ϵ model, the conservation of protection patterns between the P and P/E sites suggests that under conventional buffer conditions the ϵ module of the movable domain has slipped into the E site on the 50 S subunit. This situation induced by non-physiological buffer conditions may seem again reminiscent to a hybrid site. However, the hybrid site model does not propose a movable domain and thus would predict alternative patterns for P/P and P/E sites.

The α-ϵ model suggests that movement of the tRNAs occurs simultaneously on both large and small subunit in a co-coordinated fashion. Our observation of similar contacts between P/P and P/E indicates that the mutual arrangement of the α and ϵ regions of the movable domain may differ in parts substan-

TABLE IV

Contact sites with tRNA phosphates at the P site that were strongly protected in two different elongator tRNAs, namely $tRNA^{Phe}$ and $tRNA_m^{Met}$ (see also Fig. 6)

nt, nucleotidyl residue; aa, aminoacyl residue; Eubact., eubacterial domain; 3 domains, the eubacterial, archeal and eukaryotic domains. The conservation data concerning rRNA were obtained from the Gutell Lab Pages (www.rna.icmb.utexas.edu/csi), the sequences of the ribosomal proteins (r-prot.) are from the Sequence Retrieval System (www.expasy.ch/srs5/), the alignment followed (36) according to prodes.toulouse.inra.fr/multalin/multalin.html.

5′-Phosphate of tRNA base	Residue of rRNA or r-protein nearer than 10 Å [rRNA/nt or r-prot/aa]	Evolutionary conservation	
		Eubact.	3 domains
Y11	**23 S**/1909, 1910	80–90, ≥95	<80, 90–95
	1923, 1924	≥95, ≥95	≥95, <80
G30	**16 S**/1230	≥95	80–90
	S13/Lys-121	Lys or Arg at position 120	
Y32	**16 S**/1341	≥95	≥95
	S9/Ser-126, Lys-127, Arg-128	126 and 127: ~50% conserved 128: ~90% conserved	
G34	(anticodon: **16 S**/1400)		
C41	**16 S**/1339, 1340	≥95, <80	≥95, <80
T54	**23 S**/2280, 2327	≥95, ≥95	80–90, <80
C56	**L5**/Arg-56 and Glu-65	Arg or Lys at position 56 Arg or Lys at position *64*	
A58	protected via tertiary folding of tRNA		
U59	protected via tertiary folding of tRNA		
Y60	protected via tertiary folding of tRNA		

tially, when moving between PRE and POST states. Although tRNAs in the PRE and POST states display a similar mutual arrangement relative to each other (the angles between the tRNAs are 39° and 35° in the PRE and POST state, respectively (Ref. 12)), the positions of the CCA ends differ dramatically. Prior to translocation the CCA ends of the two tRNAs present at A and P sites are directly adjacent at the peptidyl-transferase center, an obvious requirement for peptide-bond formation. Following translocation the CCA ends are separated by over 50 Å (10, 12); after formation of the peptide bond, there is no requirement that the CCA ends remain together. This finding indicates that the postulated α region and ϵ region do not move strictly side-by-side during translocation.

Because the protection patterns encompass the entire tRNA, from the anticodon loop to the acceptor stem, a contiguous structure spanning the intersubunit space, from the decoding center to the peptidyl-transferase center, should exist. A potential structure has been identified, termed bridge B2a, in 70 S ribosomes (27). A major component of bridge B2a is the universally conserved stem-loop of H69 of 23 S rRNA, which has been proposed to undergo conformational change upon subunit association, enabling it to bridge the intersubunit space and to make contacts with both A and P site tRNAs (4). Other candidates for the movable domain include the upper region of the h44 of the 16 S rRNA (33) and parts of the ribosomal protein L2 (34, 35).

Codon-Anticodon Interaction at the P Site Is a Prerequisite for 30 S-tRNA Contacts within the 70 S Ribosome—Although representing only one of many findings presented in this paper, we believe the implications of this section are worthy of emphasis. Specifically, when the protection pattern of a P site tRNA bound to a non-programmed 70 S ribosome (*i.e.* no mRNA) was assessed, to our surprise the 30 S subunit did not contribute to the protection pattern at all (Fig. 5), whereas the 50 S pattern was similar to that observed with programmed 70 S ribosomes (Fig. 4). This result suggests that codon-anticodon interaction at the ribosomal P site of 70 S ribosomes is essential for 30 S contacts and that the additional 30 S contacts, those outside of the anticodon, are not available in the absence of codon-anticodon interaction. This finding agrees with and extends a previous observation that 30 S subunits in the absence of mRNA do not bind any tRNA at Mg^{2+} concentrations that are well suited for protein synthesis (18). Furthermore, this result implies that the 30 S subunit undergoes a conformation change upon codon-anticodon interaction, resulting in additional contacts that further stabilize the P site tRNA.

Conclusions—The conformation of a tRNA in solution depends on the buffer conditions. Under *in vivo* near conditions (polyamine buffer), the conformation differs from that observed under conventional buffer systems regardless of whether the $[Mg^{2+}]$ is 10 or 20 mM. However, the buffer systems have only little influence on the accessibility of the tRNA phosphates if the tRNA is bound to the P site. An analysis of our findings led to the following conclusions. 1) A comparison of the contact patterns of two different elongator tRNAs at the P site of programmed 70 S ribosome identified 10 common and highly protected sites that might be of strategic importance for the fixation of a tRNA at the P site. 2) The accessibility or contact patterns of the tRNAs with the isolated subunits in the presence of mRNA can be combined to produce the pattern seen at the P site of 70 S ribosomes, thus allowing a sharp delineation of the regions of a tRNA in contact with the 30 and 50 S subunits within the programmed 70 S ribosome. 3) The contact pattern of non-programmed 70 S ribosomes is almost identical to that of isolated 50 S subunits, indicating that codon-anticodon interaction at the P site is required for 30 S contacts with the tRNA. (4) On the basis of our results, we propose the following scheme for conformational rearrangements within 70 S ribosomes upon subunit association and P site tRNA binding. (i) Upon association of the ribosomal subunits forming the 70 S ribosome, the tRNA carrier of the 50 S subunit shifts from the E site to the P site. (ii) Binding a tRNA to the P site in the presence of mRNA establishes codon-anticodon interaction. This in turn induces a conformational change of the 30 S subunit that allows further stabilizing interaction with this subunit, in addition to those already existing with the 50 S subunit, both of which may be important for subsequent translocation. The presence of movable domains supports the α-ϵ model for the ribosomal elongation cycle.

Acknowledgment—We thank Sean Connell for help and discussions.

REFERENCES

1. Schluenzen, F., Tocilj, A., Zarivach, R., Harms, J., Gluehmann, M., Janell, D., Bashan, A., Bartels, H., Agmon, I., Franceschi, F., and Yonath, A. (2000) *Cell* **102,** 615–623
2. Wimberly, B. T., Brodersen, D. E., Clemons, W. M., Morgan-Warren, R. J., Carter, A. P., Vonrhein, C., Hartsch, T., and Ramakrishnan, V. (2000) *Nature* **407,** 327–339
3. Ban, N., Nissen, P., Hansen, J., Moore, P. B., and Steitz, T. A. (2000) *Science* **289,** 905–920

4. Harms, J., Schlunzen, F., Zarivach, R., Bashan, A., Gat, S., Agmon, I., Bertels, H., Franceschi, F., and Yonath, A. (2001) *Cell* **107,** 679–688
5. Pioletti, M., Schlunzen, F., Harms, J., Zarivach, R., Gluhmann, M., Avila, H., Bashan, A., Bartels, H., Auerbach, T., Jacobi, C., Hartsch, T., Yonath, A., and Franceschi, F. (2001) *EMBO J.* **20,** 1829–1839
6. Carter, A. P., Clemons, W. M., Jr., Brodersen, D. E., Morgan-Warren, R. J., Hartsch, T., Wimberly, B. T., and Ramakrishnan, V. (2001) *Science* **291,** 498–501
7. Brodersen, D. E., Clemons, W. M., Carter, A. P., Morgan-Warren, R. J., Wimberly, B. T., and Ramakrishnan, V. (2000) *Cell* **103,** 1143–1154
8. Ogle, J. M., Brodersen, D. E., Clemons, W. M., Jr., Tarry, M. J., Carter, A. P., and Ramakrishnan, V. (2001) *Science* **292,** 897–902
9. Nissen, P., Hansen, J., Ban, N., Moore, P. B., and Steitz, T. A. (2000) *Science* **289,** 920–930
10. Yusupov, M. M., Yusupova, G. Z., Baucom, A., Lieberman, K., Earnest, T. N., Cate, J. H., and Noller, H. F. (2001) *Science* **292,** 883–896
11. Yusupova, G. Z., Yusupov, M. M., Cate, J. H., and Noller, H. F. (2001) *Cell* **106,** 233–241
12. Agrawal, R. K., Spahn, C. M. T., Penczek, P., Grassucci, R. A., Nierhaus, K. H., and Frank, J. (2000) *J. Cell Biol.* **150,** 447–459
13. Döring, T., Mitchell, P., Osswald, M., Bochkariov, D., and Brimacombe, R. (1994) *EMBO J.* **13,** 2677–2685
14. Joseph, S., and Noller, H. F. (1996) *EMBO J.* **15,** 910–916
15. Joseph, S., and Noller, H. F. (1998) *EMBO J.* **17,** 3478–3483
16. Dabrowski, M., Spahn, C. M. T., and Nierhaus, K. H. (1995) *EMBO J.* **14,** 4872–4882
17. Bommer, U., Burkhardt, N., Jünemann, R., Spahn, C. M. T., Triana-Alonso, F. J., and Nierhaus, K. H. (1996) in *Subcellular Fractionation: A Practical Approach* (Graham, J., and Rickwoods, D., eds) pp. 271–301, IRL Press at Oxford University Press, Oxford
18. Gnirke, A., and Nierhaus, K. H. (1986) *J. Biol. Chem.* **261,** 14506–14514
19. Dabrowski, M., Spahn, C. M. T., Schäfer, M. A., Patzke, S., and Nierhaus, K. H. (1998) *J. Biol. Chem.* **273,** 32793–32800
20. Eckstein, F., and Gish, G. (1989) *Trends Biochem. Sci.* **14,** 97–100
21. Schnitzer, W., and Ahsen, U. V. (1997) *Proc. Natl. Acad. Sci. U. S. A.* **94,** 12823–12828
22. Agrawal, R. K., Penczek, P., Grassucci, R. A., Burkhardt, N., Nierhaus, K. H., and Frank, J. (1999) *J. Biol. Chem.* **274,** 8723–8729
23. Nierhaus, K. H., Spahn, C. M. T., Burkhardt, N., Dabrowski, M., Diedrich, G., Einfeldt, E., Kamp, D., Marquez, V., Patzke, S., Schäfer, M. A., Stelzl, U., Blaha, G., Willumeit, R., and Stuhrmann, H. B. (2000) in *The Ribosome: Structure, Function, Antibiotics, and Cellular Interactions* (Garrett, R. A., Douthwaite, S. R., Liljas, A., Matheson, A. T., Moore, P. B., and Noller, H. F., eds) pp. 319–335, ASM Press, Washington, D. C.
24. Rheinberger, H. J., and Nierhaus, K. H. (1987) *J. Biomol. Struct. Dyn.* **5,** 435–446
25. Triana-Alonso, F. J., Dabrowski, M., Wadzack, J., and Nierhaus, K. H. (1995) *J. Biol. Chem.* **270,** 6298–6307
26. Quigley, G. J., Teeter, M. M., and Rich, A. (1978) *Proc. Natl. Acad. Sci. U. S. A.* **75,** 64–68
27. Gabashvili, I. S., Agrawal, R. K., Spahn, C. M. T., Grassucci, R. A., Svergun, D. I., Frank, J., and Penczek, P. (2000) *Cell* **100,** 537–549
28. Carter, A. P., Clemons, W. M., Brodersen, D. E., Morgan-Warren, R. J., Wimberly, B. T., and Ramakrishnan, V. (2000) *Nature* **407,** 340–348
29. Hartz, D., McPheeters, D. S., and Gold, L. (1989) *Genes Dev.* **3,** 1899–1912
30. Kirillov, S. V., Makarov, E. M., and Semenkov, Y. P. (1983) *FEBS Lett.* **157,** 91–94
31. Moazed, D., and Noller, H. F. (1989) *Nature* **342,** 142–148
32. Nierhaus, K. H. (1996) in *Ribosomal RNA and Group I Int* (Green, R., and Schroeder, R., eds) pp. 69–81, R. G. Landes Co., Georgetown, TX
33. VanLoock, M. S., Agrawal, R. K., Gabashvili, I. S., Qi, L., Frank, J., and Harvey, S. C. (2000) *J. Mol. Biol.* **304,** 507–515
34. Diedrich, G., Spahn, C. M. T., Stelzl, U., Schäfer, M. A., Wooten, T., Bochariov, D. E., Cooperman, B. S., Traut, R. R., and Nierhaus, K. H. (2000) *EMBO J.* **19,** 5241–5250
35. Willumeit, R., Forthmann, S., Beckmann, J., Diedrich, G., Ratering, R., Stuhrmann, H. B., and Nierhaus, K. H. (2001) *J. Mol. Biol.* **305,** 167–177
36. Corpet, F. (1988) *Nucleic Acids Res.* **16,** 10881–10890